Title

Discovery of enzymes for toluene synthesis from anoxic microbial communities

Journal

Nature Chemical Biology, 14(5)

ISSN

1552-4450

Authors

Beller, Harry R

Rodrigues, Andria V

Zargar, Kamrun

et al.

Publication Date

2018-05-01

DOI

10.1038/s41589-018-0017-4

Peer reviewed

Enzyme discovery for toluene synthesis in anoxic microbial communities

H. R. Beller†*[1,2], A. V. Rodrigues†[1], K. Zargar†[1], Y.-W. Wu[3], A. K. Saini[1], R. M. Saville[1], J. H. Pereira[1], P. D. Adams[1], S. G. Tringe[4], C. J. Petzold[1,5], J. D. Keasling[1,5,6,7]

Joint BioEnergy Institute, 5885 Hollis Avenue, Emeryville, CA, USA[1]; Earth and Environmental Sciences, LBNL, Berkeley, CA, USA[2]; Graduate Institute of Biomedical Informatics, College of Medical Science and Technology, Taipei Medical University, Taipei, Taiwan[3]; Joint Genome Institute, 2800 Mitchell Drive, Walnut Creek, CA, USA[4]; Biological Systems and Engineering, Lawrence Berkeley National Laboratory (LBNL), Berkeley, CA, USA[5]; Departments of Chemical & Biomolecular Engineering and of Bioengineering, University of California, Berkeley, CA, USA[6]; Novo Nordisk Foundation Center for Biosustainability, Technical University of Denmark, Kogle Allé, DK2970-Hørsholm, Denmark[7]

†These authors contributed equally to this work.

* Corresponding author: HRBeller@lbl.gov

Microbial toluene biosynthesis was reported in anoxic lake sediments more than 3 decades ago, however the enzyme(s) catalyzing this biochemically challenging reaction have never been elucidated. Here we report the first toluene synthase, a glycyl radical enzyme of bacterial origin that catalyzes phenylacetic acid decarboxylation (PhdB), and its cognate activating enzyme (PhdA, a radical *S*-adenosylmethionine enzyme), discovered in two distinct anoxic microbial communities that produced toluene. The unconventional process of enzyme discovery from a complex microbial community (>300,000 genes) rather than from a microbial isolate, involved metagenomics- and metaproteomics-enabled biochemistry, as well as *in-vitro* confirmation of activity with recombinant enzymes. This work expands the known catalytic range of glycyl radical enzymes (only seven reaction types had been characterized previously) and aromatic hydrocarbon-producing enzymes (only one reaction type characterized previously), and will enable first-time biochemical synthesis of an aromatic fuel hydrocarbon from renewable resources, such as lignocellulosic biomass, rather than petroleum.

The extraordinary metabolic diversity of microorganisms in combination with ready access to increasingly rapid and less expensive DNA sequencing technologies has revealed a well-recognized challenge in modern biology: the dearth of experimental evidence to support functional annotation of a large fraction of genes/proteins in public data repositories[1-3]. A related challenge, termed "orphan enzymes"[4], is the abundance of unambiguously defined enzymatic activities that are not linked with specific amino acid sequences; in 2014, 22% of defined EC (Enzyme Commission) numbers were orphan enzymes[5]. To the extent that specific enzymes can be better linked to a broad range of chemically diverse reactions, the scope and versatility of

biochemical transformations harnessed for biotechnological applications will be enhanced. One area in which knowledge of enzymes is very limited is biosynthesis of aromatic hydrocarbons, which could be useful as renewable fuels or chemicals made from non-petroleum feedstocks. To our knowledge, the only aromatic hydrocarbon that can currently be synthesized wholly from known enzymes is styrene, which can be produced from phenylalanine-derived *trans*-cinnamic acid by enzymes displaying phenylacrylate decarboxylase activity, such as ~~PAL2 from *Arabidopsis thaliana* or~~ FDC1 from *Saccharomyces cerevisiae*[6].

We targeted the aromatic hydrocarbon toluene for enzyme discovery, as it is an important petrochemical with a global market of 29 million tons per year whose uses include synthesis of other aromatic feedstocks and serving as an effective octane booster in gasoline (octane number, 114). Microbial sources of biogenic toluene were reported more than three decades ago, however, the underlying biochemistry and specific enzymes catalyzing toluene biosynthesis have never been elucidated. Biogenic toluene was observed in anoxic lake sediments / hypolimnion[7], in anoxic enrichment cultures derived from municipal sewage sludge[8], and in two bacterial isolates, *Tolumonas auensis*[9] and *Clostridium aerofoetidum*[10], which were reported to synthesize toluene from phenylacetate and L-phenylalanine (however, recent attempts to reproduce toluene biosynthesis by these two isolates were unsuccessful[8]). Although a toluene synthase has not been specifically identified, *in vitro* studies with cell-free extracts from a toluene-producing culture suggest catalysis by a glycyl radical enzyme (GRE)[8]. Evidence supporting the hypothesized role of a GRE in toluene biosynthesis included (a) irreversible inactivation by O_2 (a characteristic of GREs), (b) the ruling out of a mechanism involving successive reduction (phenylacetate to phenylacetaldehyde) and decarbonylation/deformylation (phenylacetaldehyde to toluene), which would not be expected to be catalyzed by GREs[11,12], and (c) the observation that the known

enzyme with the greatest functional similarity to phenylacetate decarboxylase, namely *p*-hydroxyphenylacetate decarboxylase (HpdBC or CsdBC), is a GRE[13,14]. Although a GRE has been implicated in toluene biosynthesis, even the most detailed *in vitro* studies conducted to date have not identified any specific gene candidates[8].

Identification of toluene synthase candidates

Studies to identify a toluene synthase (phenylacetate decarboxylase) were conducted with anaerobic, toluene-producing microbial cultures that derived from two different inocula: municipal sewage sludge[8] and lake sediments from Berkeley, CA (Extended Data Fig. 1). The sewage culture, which was more amenable to cultivation and *in vitro* studies, served as the basis for most of the experimental discovery studies, whereas the lake sediment culture was used primarily for metagenome sequencing. We employed a metagenomics- and metaproteomics-enabled protein purification approach for enzyme discovery from these microbial communities. Toluene synthase activity was monitored in chromatographically separated fractions of cell-free extracts from the sewage culture using *in vitro* assays that measured phenylacetic acid-2-^{13}C conversion to [*methyl*-^{13}C]toluene. All experimental procedures, including cultivation, cell lysis, protein purification by FPLC (fast protein liquid chromatography), and *in vitro* assays, were performed under strictly anaerobic conditions to protect the organisms and enzymes from molecular oxygen. Proteomic profiles of active FPLC fractions were compared to those of adjacent inactive (or much less active) fractions to identify toluene synthase candidates (i.e., those proteins enriched in, and ideally unique to, active fractions). An unknown GRE (hereafter referred to as PhdB) co-eluted with the maximal toluene synthase activity (Extended Data Fig. 2). Although more than 650 proteins co-eluted with PhdB in these fractions (Supplementary Data File 1), this protein was initially of interest because the toluene synthase in this sewage-

derived culture had been postulated to be a GRE based upon *in vitro* studies with cell-free extracts[8]. Notably, PhdB was one of the few glycyl radical enzymes detected in active fractions among the many glycyl radical enzymes encoded in the sewage community metagenome (Fig. 1). As shown in Fig. 1, only three glycyl radical enzymes were detected in the active FPLC fractions: (1) PhdB, (2) pyruvate formate-lyase (PflB; JGI2065J20421_100036324; IMG Taxon ID 3300001865), which had 99% sequence identity to known *Enterobacter* PflB copies], and (3) an unknown glycyl radical enzyme (JGI2065J20421_10067673; IMG Taxon ID 3300001865) – this protein shares ca. 47% sequence identity and key conserved residues with a known glycerol dehydratase (PDB 1R8W). Of these three proteins, only PhdB and the PflB had greater abundance in active than in flanking inactive fractions (Fig. 1), and PflB was among the most abundant proteins in both active *and* inactive fractions (Supplementary Data File 1), which, along with its well-characterized function, reduced its plausibility as a toluene synthase candidate.

The strength of *phdB* as a candidate toluene synthase gene was enhanced by its identification in metagenomes of both the anoxic, toluene-producing sewage and lake sediment cultures, despite the fact that these cultures had disparate inocula and phylogenetic compositions (a comparison of dominant taxa in these two cultures is shown in Extended Data Fig. 3 and Supplementary Data Files 2 and 3). In sewage culture metagenomes, *phdB* occurred in a three-gene cluster consisting of a putative transcription factor (Sequence 11, Supplementary Data File 4), *phdB* (Sequence 6, Supplementary Data File 4), and a glycyl radical activating enzyme (hereafter referred to as *phdA*; Sequence 1, Supplementary Data File 4) (Fig. 2). Such adjacent positioning in genomes of genes encoding glycyl radical enzymes and their cognate activating enzymes is very common[15], as indicated in Fig. 2. Although assembled contigs from the lake

sediment metagenomes (e.g., IMG Taxon ID 2100351000) were not observed to harbor the complete three-gene cluster detected in the sewage metagenome, the quality of these assemblies was suboptimal as a result of older sequencing methods used. Indeed, PCR amplification and Sanger sequencing of this cluster from genomic DNA of the lake culture revealed an intact three-gene cluster (Sequence 13-Sequence 9-Sequence 4; Supplementary Data File 4) with identical length (6065 bp) and strikingly similar coding and intergenic sequences compared to the sewage culture (Fig. 2). As shown in Fig. 2, the three genes share from ca. 87 to 96% sequence identity (and 86 to 97% translated sequence identity) in the sewage and lake cultures and the intergenic regions are ca. 82-85% identical (Sequences 15 and 16; Supplementary Data File 4).

In vitro confirmation of PhdB and PhdA activity

Recombinant versions of PhdA and PhdB were assayed for *in vitro* activity to confirm their role in catalyzing toluene biosynthesis from phenylacetate. The expected activity for PhdA was based on characterization of other glycyl radical activating enzymes[16]. In glycyl radical systems, the reduced $[4Fe\text{-}4S]^{+1}$ cluster of the activase, a radical *S*-adenosylmethionine (SAM) enzyme, transfers an electron to SAM, resulting in homolytic cleavage of SAM to form methionine and a 5'-deoxyadenosyl radical (Fig. 3a). The 5'-deoxyadenosyl radical activates the GRE by stereospecific abstraction of a C-2 *pro-S* H atom from a highly conserved glycine residue, which in turn abstracts an H atom from a conserved cysteine residue in the GRE to form a thiyl radical. A substrate radical is formed when the thiyl radical abstracts an H atom from the substrate (phenylacetic acid, in the case of PhdB; Fig. 3b).

In vitro reconstitution of the [4Fe-4S] cluster of PhdA was performed before final purification (all under strictly anaerobic conditions), and the [4Fe-4S] cluster was reduced with dithionite in an ~~anaerobic~~ anoxic assay measuring methionine production from SAM using liquid

chromatography-mass spectrometry (LC/MS). Observed methionine production in the presence of PhdA, but not in its absence (Fig. 3a), demonstrated the expected activity of a glycyl radical activating enzyme.

The ability of activated (enzyme-radical) PhdB to catalyze decarboxylation of phenylacetic acid-2-^{13}C to [*methyl*-^{13}C]toluene was tested in an ~~anaerobic~~anoxic, *in vitro* assay in the presence of dithionite-reduced PhdA and SAM (Fig. 3b). Labeled toluene was detected by gas chromatography-mass spectrometry (GC/MS) in the presence of SAM but not in its absence, confirming the role of PhdB in catalyzing toluene biosynthesis *via* a radical mechanism. A series of other negative control assays also displayed negligible activity, including the following: (1) assays lacking PhdB but containing dithionite-reduced PhdA and SAM, (2) assays conducted with a mutant version of PhdB (G815A) in which the putative site of the glycyl radical was modified to alanine, and (3) assays in which the assay mixture was briefly exposed to air before the substrate was added, demonstrating O_2 sensitivity that is characteristic of GREs (Extended Figure 4). Specific activities observed in SAM-containing assays represented in Figure 3b were relatively low (in the pmol · min^{-1} · mg protein^{-1} range) compared to reported values for most other GREs, which range broadly from pmol · min^{-1} · mg protein^{-1} (benzylsuccinate synthase[17]) to mmol · min^{-1} · mg protein^{-1} (glycerol dehydratase[18]). In part, low PhdB activity may reflect the generally sensitive nature of GREs when purified and manipulated *in vitro*. For example, even for a given enzyme, reported specific activities have differed by orders of magnitude in various studies [e.g., for benzylsuccinate synthase, from 0.02[17] to 72 nmol · min^{-1} · mg protein^{-1} [19]; for *p*-hydroxyphenylacetate decarboxylase, from 0.034[13] to 18.45 µmol · min^{-1} · mg protein^{-1} [14]]. In the present study, a likely factor affecting PhdB activity was the poor solubility of the recombinant protein when expressed in *E. coli* (Extended Figure 5); a maltose-binding protein (MBP) tag was

used to enhance solubility but may not have fully ameliorated suboptimal folding. For biotechnological application of PhdB, enhanced solubility (e.g., through protein engineering) will be required.

While PhdB displays phenylacetate decarboxylase activity, it does not display comparable *p*-hydroxyphenylacetate decarboxylase activity (characteristic of the GRE HpdBC/CsdBC). During assays in which equimolar amounts of phenylacetate and *p*-hydroxyphenylacetate were amended to a mixture containing PhdA, PhdB, and SAM, labeled toluene production was readily observed, however, *p*-cresol (the product of *p*-hydroxyphenylacetate decarboxylation) was detected at levels approximately 100-fold lower than those expected if PhdB activity were comparable for phenylacetate and *p*-hydroxyphenylacetate (Extended Data Fig. ~~4~~6). Analogous assays with *o*- and *m*-hydroxyphenylacetate similarly indicated very low (in this case, undetectable) PhdB activity for these hydroxyphenylacetate isomers, whereas labeled toluene was easily detected.

Comparison of PhdB-PhdA to other glycyl radical systems

The demonstration of PhdB as a phenylacetate decarboxylase adds it to the group of seven characterized GREs (Fig. 4), which includes pyruvate formate-lyase (EC 2.3.1.54[20]), anaerobic ribonucleotide reductase (EC 1.17.4.1[21]), benzylsuccinate synthase (EC 4.1.99.11[17,19,22]), *p*-hydroxyphenylacetate decarboxylase (EC 4.1.1.82[13,14,23]), B_{12}-independent glycerol (and 1,2-propanediol) dehydratase (EC 4.2.1.30[18]), choline trimethylamine-lyase (EC 4.3.99.4[24,25]), and the very recently discovered *trans*-4-hydroxy-L-proline dehydratase[26]. Note that benzylsuccinate synthase, which catalyzes the first step of anaerobic toluene degradation, is the best characterized representative of a larger group of aromatic- and alkylsuccinate synthase

enzymes that activate substrates including 2-methylnaphthalene, *p*-cresol, and *n*-hexane by fumarate addition and have been collectively termed "X-succinate synthases"[27].

PhdB shares important features characteristic of all known GREs, including the following: (1) a conserved glycyl radical motif (RVx**G**[FWY]x_{6-8}[*I*L]x_4Qx_2[IV]x_2R — modification from Selmer et al.[15] indicated in italics) near the C-terminus of the protein (Fig. 5a), (2) a conserved cysteine residue near the middle of the protein sequence (the site of the thiyl radical in the active site that initiates H atom abstraction from the substrate) (Fig. 5b), and (3) a cognate activating enzyme that belongs to the radical SAM superfamily[15]. However, PhdB is clearly distinct from the other known glycyl radical enzymes in a number of ways. For example, the sequence identity of PhdB (from the sewage and lake cultures) to other GREs is relatively low, ranging from ca. 14 to 31% (Extended Data Fig. 7~~5~~). Further, PhdB does not share all of the conserved residues that have been assigned for other GREs. To illustrate, in the region near the conserved active-site C residue (Fig. 5b), some conserved residues not shared by PhdB include an additional C adjacent to the strictly conserved active-site C (PflB[20]), an E located two residues downstream of the active-site C (CsdB[23], Gdh[18], CutC[24], HypD[26]), and M-S-P residues immediately downstream of the active-site C (BssA[27]).

With respect to *p*-hydroxyphenylacetate decarboxylase in particular, differences from PhdB are noteworthy, since these proteins might be expected to be very similar based on the seemingly analogous reactions that they catalyze (Fig. 4). Phenylacetate decarboxylase (PhdB) has only one subunit type, in contrast to *p*-hydroxyphenylacetate decarboxylase (CsdBC or HpdBC), which has two (Fig. 2), and does not share conserved CsdB residues postulated to interact with the *para*-hydroxy group (e.g., active-site residue E637 of CsdB[23]). Furthermore, *p*-hydroxyphenylacetate decarboxylase (CsdBC) does not act on phenylacetate[8], and conversely,

PhdB has far lower activity on *p*-hydroxyphenylacetate than on phenylacetate (Extended Data Fig. 6). Based upon the sole structural feature that differentiates the substrates of PhdB and *p*-hydroxyphenylacetate decarboxylase (CsdBC/HpdBC), namely a *para*-hydroxy group, and its essential role in the proposed mechanism of the latter enzyme, it is likely that PhdB and CsdBC/HpdBC differ mechanistically. The Kolbe-type decarboxylation proposed for CsdBC[23,28] involves an unprecedented mechanism for *p*-hydroxyphenylacetate activation: a concerted abstraction of a proton from the *para*-hydroxy group by E637 and abstraction of an electron from the carboxyl group by C503[23]. Together, the proton and electron abstraction constitute a *de facto* H-atom abstraction, although the abstraction occurs in two distinct locations on the substrate molecule. Molecular modeling of the substrate-bound active sites of PhdB (based on homology modeling) and CsdBC (based on crystallographic data) indicates important conserved residues, such as the sites of the thiyl radical (C482 in PhdB and C503 in CsdB) and glycyl radical (G815 in PhdB and G873 in CsdB), but also important differences, such as a hydrophobic pocket in PhdB (including W495, Y691, and V693) accommodating the unsubstituted ring of phenylacetate and lacking the H536 and E637 residues in CsdB that are proposed to interact with the *para*-hydroxy group of *p*-hydroxyphenylacetate (Extended Figure 8).

Just as PhdB represents a novel glycyl radical enzyme, PhdA represents a new glycyl radical activating enzyme. Whereas PhdA shares some characteristics of the cognate activating enzymes for the seven GREs described above, such as a conserved CxxxCxxC [4Fe-4S]-binding motif near the N-terminus of the protein (Fig. 5c), its sequence identity to these activating enzymes is relatively low (from ca. 23 to 42% for both the sewage and lake culture versions of PhdA; Extended Data Fig. 7). To date, studies have indicated that glycyl radical activating enzymes are not interchangeable but rather are specific to their cognate glycyl radical enzymes[16].

Identity of toluene-producing bacterium

As toluene synthase discovery was conducted with the proteome of a complex microbial community rather than that of a microbial isolate, the task of identifying the microbe whose genome encodes *phdA* and *phdB* was challenging. Nonetheless, we were able to recover the draft genome of the bacterium in the sewage community that putatively expressed *phdA* and *phdB* (Fig. 6a). This 3.61-Mbp genome (Fig. 6a, Supplementary Data File 5), which resulted from co-assembly of Illumina reads from multiple metagenome sequences produced from the sewage culture, is estimated to be 96.35% complete and contains a 51.8-kb contig including the three-gene *phd* cluster (Fig. 2) relevant to toluene biosynthesis. In addition to *phdA* and *phdB*, the genome encodes other putative radical-related enzymes (Fig. 6a), including a GRE of unknown function (TOLSYN_01027) and seven putative radical SAM enzymes that contain the CxxxCxxC motif near the N terminus (TOLSYN_00781, TOLSYN_01308, TOLSYN_01024, TOLSYN_00072, TOLSYN_00941, TOLSYN_02430, and TOLSYN_01488).

The recovered genome contained a partial 16S rRNA gene indicating that the toluene-producing bacterium (hereafter referred to as *Acidobacteria* strain Tolsyn) belongs to the *Acidobacteria* phylum (Extended Data Fig. 96). The closest match among bacterial isolates is to *Candidatus* Koribacter versatilis (95% identity), which is classified in Subdivision 1 of the *Acidobacteria* but is not well characterized with respect to its physiology and metabolism[29]. Evaluation of the recovered genome against the available *Acidobacteria* isolate genomes using 129 concatenated proteins (including 33 ribosomal proteins) indicated, as did the 16S rRNA analysis, that the closest isolated relative is *Ca.* Koribacter versatilis (Fig. 6b). However, the genomes of *Acidobacteria* strain Tolsyn and *Ca.* Koribacter versatilis are much less similar than the 16S rRNA comparison would suggest: average sequence identity for the proteins in these two

genomes was only ca. 56%. Admittedly, there are few *Acidobacteria* isolates for comparison to strain Tolsyn, as *Acidobacteria* are notoriously difficult to isolate[29,30]. Notably, BLASTP[31] searches of the *Ca.* Koribacter versatilis genome did not yield any hits to PhdA or PhdB.

From an ecological perspective, the selective advantage conferred by toluene production in strain Tolsyn is currently unknown. The metabolic advantages rendered by phenylacetate conversion to toluene are not obvious, as the reaction yields only CO_2, which is unlikely to be limiting in environments like anoxic lake sediments or sewage sludge, and toluene, which is likely lost from the cell by diffusion and not further metabolized [e.g., benzylsuccinate synthase[22] was not found in the genome nor, indeed, in the entire sewage metagenome (IMG Taxon ID 2633300001865)]. ~~Further, the PhdB reaction will not provide reducing equivalents to the host because it is not an oxidation-reduction reaction.~~ Here, we present two possible explanations for the selective advantage offered by toluene biosynthesis. ~~By~~ First, by analogy to *p*-hydroxyphenylacetate decarboxylation to *p*-cresol, as catalyzed by the nocosomial pathogen *Peptoclostridium difficile* (formerly *Clostridium difficile*), it is possible that toluene production represents a form of negative allelopathy. In *P. difficile*, production of the bacteriostatic agent *p*-cresol is thought to provide a competitive advantage to the producing strain and has been proposed as a virulence factor[32]. Just as the ultimate source of *p*-hydroxyphenylacetate to *P. difficile* is tyrosine metabolism, the source of phenylacetate to strain Tolsyn is likely phenylalanine metabolism[8], potentially involving transamination of phenylalanine to phenylpyruvate (e.g., *via* phenylalanine transaminase; EC 2.6.1.57), decarboxylation to phenylacetaldehyde (e.g., *via* phenylpyruvate decarboxylase; EC 4.1.1.43), and oxidation to phenylacetate (e.g., *via* phenylacetaldehyde dehydrogenase; EC 1.2.1.39)[33], although other pathways are possible[34]. Notably, BLASTP searches of the *Acidobacteria* strain Tolsyn genome

did not reveal definitive copies of genes encoding any of these enzymes, suggesting that the conversion of phenylalanine to phenylacetate may not occur within strain Tolsyn, but rather that phenylacetate may be imported from its environment. Regardless of which microorganisms are converting phenylalanine to phenylacetate, previous studies have documented that the conversion of labeled phenylalanine (L-phenylalanine-β-^{13}C) to labeled toluene ([*methyl*-^{13}C]toluene) definitively occurs in this sewage culture[8].

The prospect of phenylacetate import into *Acidobacteria* strain Tolsyn introduces a second possible explanation for the selective advantage offered by toluene biosynthesis: intracellular pH homeostasis and/or development of a proton motive force (pmf). If the anion phenylacetate were imported into the cell, the PhdB-catalyzed decarboxylation to toluene consumed a proton from the cytoplasm (consistent with the balanced reaction of $C_8H_7O_2^- + H^+ \rightarrow C_7H_8 + CO_2$), and the neutral reaction products toluene and CO_2 (or H_2CO_3) exited the cell (e.g., by diffusion), the result would be alkalinization of the cytoplasm and indirect development of a pmf (by depletion of protons from the cytoplasm rather than the canonical pumping of protons across the cytoplasmic membrane). Studies of tyrosine and histidine decarboxylation in *Enterococcus* and *Lactobacillus* spp. have experimentally supported analogous mechanisms for pmf development and intracellular pH regulation[35,36]. Thus, alkalinization of the cytoplasm *via* phenylacetate decarboxylation could promote tolerance to the moderately acidic conditions characteristic of some fermentative environments (such as those used to cultivate the sewage and lake sediment cultures and likely representative of their native habitats) and could also provide a source of energy to the bacterium (as pmf), even though the PhdB reaction would not provide reducing equivalents to the host because it is not an oxidation-reduction reaction.

Conclusion

We have discovered a GRE that catalyzes an activity heretofore unavailable to biotechnology, enabling biochemical synthesis of toluene (and potentially other products of aromatic acid decarboxylation) from renewable feedstocks. Furthermore, this study, like the recent discovery of another GRE (*trans*-4-hydroxy-L-proline dehydratase[26]), provides a glimpse into the untapped catalytic potential of GREs. It is likely that the catalytic diversity of GREs has been widely underestimated because automated annotation pipelines routinely misidentify diverse GREs as pyruvate formate-lyase (as was the case for PhdB), and there is a dearth of experimental data to correct such misannotation. To illustrate the unexplored diversity of GREs, consider the sewage-derived microbial community investigated in this study. In addition to PhdB, we conservatively estimate that there are at least four other novel GREs represented in the sewage culture metagenome (Fig. 1), as detailed in Extended Data Fig. 10~~7~~. These GREs deviate from known GREs with respect to at least one conserved residue, and share only ca. 16 to 38% protein sequence identity with known GREs and each other. All four of these putatively novel GREs were misannotated as pyruvate formate-lyase by an automated pipeline. Further experimental characterization of the catalytic range of GREs promises to expand our understanding of the metabolic diversity of anaerobic bacteria and the reach of biotechnology to catalyze challenging reactions.

METHODS

Unless stated otherwise, all cultivation and biochemical processes were conducted under strictly anaerobic conditions[37] in an anaerobic glove box (Type B, Coy Laboratory Products, Inc., Grass Lake, MI) with a nominal gas composition of 85% N_2 – 10% CO_2 – 5% H_2 (ultra-high

purity, anaerobic mixture) maintained at ambient temperature (~22°C). Glass, plastic, and stainless steel materials used to manipulate microbial cells, cell-free extracts, and purified enzymes in the glove box were allowed to degas in the anaerobic glove box for at least one day before use, as were heat-labile solids that could not be prepared in autoclaved and purged solutions. Highly purified water (18 MΩ resistance) obtained from a Barnstead Nanopure system (Thermo Scientific, Waltham, MA) was used to prepare all aqueous solutions described in this article. Chemicals used in this study were of the highest purity available and were used as received.

Cultivation of anaerobic sewage and lake sediment cultures

Anaerobic cultivation of sewage-derived cultures has been described previously[8]. In a similar fashion, reducing sediments from a lake in Berkeley, California, were used to inoculate cultures under anaerobic conditions using TP[9] or modified TP[8] growth medium in an anaerobic glove box. Amended phenylacetate (typically 200 µM) and evolved toluene were monitored by LC/MS and GC/MS, respectively, using methods described previously[8].

Partial purification of phenylacetate decarboxylase activity in sewage cultures with FPLC

As described in detail elsewhere[8], cell-free extracts from the sewage-derived culture were generated under strictly anaerobic conditions with a French pressure cell[19] (138 MPa) and clarified by ultracentrifugation, before being subjected to FPLC fractionation in an anaerobic glove box with a Bio-Scale Mini CHT-II ceramic hydroxyapatite column (5-mL bed volume, 40-µm particle diameter; Bio-Rad, Hercules, CA) and Bio-Rad Econo Gradient Pump. ~~Toluene synthase~~Phenylacetate decarboxylase activity in FPLC fractions was determined with a GC/MS static headspace assay that measured conversion of phenylacetic acid-2-^{13}C (Icon Isotopes, Summit, NJ; 99 atom% ^{13}C) to [*methyl*-^{13}C]toluene[8].

Proteomic analysis of FPLC fractions by LC/MS/MS

Details on proteomic analysis of selected FPLC fractions, including data processing, were provided by Zargar et al.[8]. Briefly, proteomic LC/MS/MS analysis was performed with a Q Exactive Orbitrap mass spectrometer (Thermo Scientific) in conjunction with a Proxeon Easy-nLC II HPLC (Thermo Scientific) and Proxeon nanospray source.

Characterization of sewage and lake cultures by next-generation sequencing of metagenomes and PCR-amplified 16S rRNA genes

Extraction of genomic DNA from toluene-producing cultures was performed with a bead-beating method involving hexadecyltrimethylammonium bromide (CTAB) extraction buffer described elsewhere[8]. Genomic DNA was purified with Allprep DNA/RNA kits (Qiagen, Valencia, CA). Methods used by the Joint Genome Institute (JGI) for metagenome library construction, next-generation sequencing (Illumina and PacBio), and assembly for sewage- and lake-derived cultures are summarized in Supplementary Data File 6, along with accession numbers for NCBI's SRA (Sequence Read Archive; https://trace.ncbi.nlm.nih.gov/Traces/sra/sra.cgi). The automated annotation pipeline for metagenome sequences was described previously[38].

Composition of the sewage-derived community was analyzed at the JGI by Illumina sequencing of 16S rRNA genes amplified from the V4 region (primers 515F and 806R). Library construction and sequencing methods are described in Supplementary Data File 6, and data analysis with iTagger v. 1.1 was performed as described previously[8].

Composition of the lake sediment-derived community was also assessed by Illumina sequencing of 16S rRNA genes amplified from the V4 region (primers 515F and 806R). Library

construction was performed according to the Earth Microbiome Project standard protocol (http://www.earthmicrobiome.org/protocols-and-standards/16s/). Sequencing was conducted by the QB3-Berkeley Core Research Facility at UC Berkeley on the Illumina MiSeq platform (San Diego, CA) with paired-end, 300-bp reads (MiSeq Reagent Kit v3, 600 cycle). The UPARSE method was used for sequence processing and operational taxonomic unit (OTU) clustering at 97% identity to process raw sequences (fastq_maxdiffs=3, fastq_trunclen=250, fastq_maxee=0.1). A set of 217 OTUs from a total of 108,041 filtered sequences were identified. For each OTU, a representative sequence was selected as described by Edgar[39]. Taxonomic assignments were made with a Naïve Bayes Classifier using the V4 region of the SILVA[40] SEED sequences and their taxonomic identities as a training set.

Cloning, expression, *in vitro* reconstitution, and purification of PhdA and PhdB

Bacterial strains and plasmids used in this study are listed in Extended Data Table 1. Strains and plasmids along with their associated information (annotated GenBank-format sequence files) have been deposited in the public version of the JBEI Registry (https://public-registry.jbei.org; entries JPUB_xxx to JPUB_xxx) and are physically available from the authors and/or addgene (http://www.addgene.org) upon request [Note to editor: JPUB names will be generated and made public upon publication of the manuscript]. Restriction enzymes were purchased from Thermo Scientific (Waltham, MA), and Phusion DNA polymerase and T4 ligase were from New England Biolabs (Ipswich, MA). Plasmid extractions were carried out using Qiagen (Valencia, CA) miniprep kits. Oligonucleotide primers were designed using the web-based PrimerBlast program (http://www.ncbi.nlm.nih.gov/tools/primer-blast/index.cgi?LINK_LOC=BlastHomeAd) and synthesized by Integrated DNA Technologies (IDT), Inc. (San Diego, CA) or Eurofins MWG Operon (Huntsville, AL).

phdA and *phdB* were codon optimized (GenScript, Piscataway, NJ) for expression in *E.coli* BL21(DE3) (listed as Sequences 3 and 8 in Supplementary Data File 4). Each codon-optimized gene was individually cloned into plasmid pET28b (Novagen, Madison, WI). *phdA* was cloned between NdeI and BamHI restriction sites (primers listed in Extended Data Table 2), resulting in a construct that encodes an N-terminal His_6-PhdA protein (pAS004; Extended Data Table 1). *phdB* was cloned between NdeI and XhoI restriction sites (primers listed in Extended Data Table 2). To enhance soluble PhdB yield, the construct also included the gene encoding maltose-binding protein (MBP) and a sequence encoding the tobacco etch virus (TEV) protease recognition site, which were inserted downstream of the N-terminal His_6 sequence and upstream of the *phdB* start codon, resulting in a construct that encodes a His_6-MBP-PhdB fusion protein with a TEV protease-cleavable His_6-MBP tag (pAS010, Extended Data Table 1). Plasmids were transformed into chemically competent *E.coli* DH10B cells grown on lysogeny broth (LB) agar plates under 50 μg/mL kanamycin selection (LB Kan-50 plates; Teknova, Hollister, CA). Plasmids were sequence-confirmed (Genewiz, South San Francisco, CA). Plasmids pAS006 (with *phdA*) and pAS010 (with *phdB*) were separately transformed into chemically competent *E.coli* BL21(DE3) cells (New England Biolabs) on LB Kan-50 plates. Transformants were grown in LB broth and stored as 100 μL glycerol stock aliquots at -80˚C.

For overexpression of PhdA, a frozen glycerol stock of strain AS013 (Extended Data Table 1) was used to inoculate 50 mL LB broth containing 50 μg/mL kanamycin (Teknova) in a 250-mL shake flask. The starter culture was incubated overnight at 30˚C with constant shaking at 200 rpm. For larger scale growth, the starter culture was diluted 100-fold in a 2-L baffled shake flask containing 1L LB broth supplemented with 50 μg/mL kanamycin, and grown aerobically at 37˚C with constant shaking (190 rpm). At OD_{600} ~0.7, the culture was induced with isopropyl β-

D-1-thiogalactopyranoside (IPTG; IBI Scientific, Peosta, IA) to a final concentration of 0.5 mM and supplemented with an aqueous solution of $Fe(NH_4)_2(SO_4)_2 \cdot 6H_2O$ (Sigma, St. Louis, MO; prepared anaerobically) to a final concentration of 200 μM. Following induction, the temperature was decreased to 18°C and the culture was propagated overnight at this temperature for ~18 hours. Cells were then harvested by centrifugation and cell pellets were stored at -80°C until lysis.

For overexpression of PhdB, strain AS019 (Extended Data Table 1) was cultivated in autoinduction medium[41]. A frozen glycerol stock was used to inoculate 50 mL ZYP-0.8G medium containing 100 μg/mL kanamycin in a 250-mL shake flask incubated overnight at 30°C with constant shaking (200 rpm). The starter culture was diluted 100-fold into a 2-L baffled shake flask containing 1-L ZYP-5052 medium with 100 μg/mL kanamycin and grown aerobically at 37°C with constant shaking at 190 rpm. At OD_{600} ~1.5, the temperature was decreased to 18°C and the culture was propagated overnight at this temperature for ~18 hours. Cells were then harvested by centrifugation and cell pellets were stored at -80°C until lysis.

All purification steps were carried out under strictly anaerobic conditions. For lysis, cells were passed three times through a French pressure cell (138 MPa) under anaerobic conditions. Sealed lysates were centrifuged under anaerobic conditions at 19,000 rpm at 4°C for 40 min. Clarified lysates were purified within an anaerobic glove box as described below using an Econo-Gradient pump coupled with a model 2110 fraction collector (Bio-Rad).

For PhdA purification, strain AS013 cell pellets were resuspended in buffer A [50 mM TRIS (pH 7.5; EMD Millipore, Billerica, MA), 300 mM NaCl (EMD Millipore), 10 mM imidazole (Sigma), 0.1 mM DL-dithiothreitol (DTT; VWR, Visalia, CA)] and mixed with powdered protease inhibitors (Pierce EDTA-free tablets, Thermo Scientific), chicken egg

lysozyme (300 μg/mL, Sigma) and DNaseI (10 μg/mL, Sigma). This mixture was incubated for 20 min followed by cell lysis and clarification of the lysate as described above. The clarified lysate was filtered through a 0.45-μm filter (EMD Millipore) and loaded onto a 5-mL HisTrap HP column (GE Healthcare, Chicago, IL) that was pre-equilibrated with buffer A. The column was then washed with 3 column volumes (CV) of buffer A to remove unbound proteins and eluted using a stepwise imidazole gradient made by mixing buffer A with buffer B [50 mM TRIS (pH 7.5), 300 mM NaCl, 500 mM imidazole, 0.1 mM DTT] using stepwise concentrations of 20 mM, 50 mM, 250 mM, and 400 mM imidazole. Each step was set to 1.6 CV and 2-mL fractions were collected. Fractions containing PhdA were dark red-brown and eluted at a concentration of 250 mM imidazole. The purity of PhdA fractions was confirmed by SDS-PAGE. Elution fractions were pooled and DTT was added to a final concentration of 2 mM. To keep the protein anoxic during concentration outside the glove box, a 10-kDa molecular weight cutoff (MWCO) concentrator (EMD Millipore) was sealed inside a 250-mL centrifuge bottle (Nalgene, Rochester, NY) with an O-ring-sealed cap. Concentrated protein was exchanged into buffer C [50 mM TRIS (pH 7.5), 300 mM NaCl, 5 mM DTT] using a pre-equilibrated PD-10 desalting column (GE Healthcare). Protein concentration was determined using the Bradford assay (Bio-Rad). Collected UV-visible spectra (UV-2450; Shimadzu Scientific, Pleasanton, CA) indicated the presence of [2Fe-2S] clusters bound to the protein (Extended Data Figure 11~~8~~)[42].

For reconstitution of [4Fe-4S] clusters in PhdA, which are required for activity, the protein was diluted to 0.2 mM in buffer C in a stoppered serum bottle and cooled to 4°C. DTT was then added to a final concentration of 10 mM and the solution was incubated at 4°C for ~1 hour. Aqueous $Fe(NH_4)_2(SO_4)_2 \cdot 6H_2O$ was added to a final concentration of 1 mM and incubated at 4°C for ~3-4 hours. Aqueous $Na_2S \cdot 9H_2O$ was then added to a final concentration of 0.9 mM

and the mixture was incubated at 4°C overnight (~18 hr). The protein mixture was then filtered through a 0.45-µm filter, concentrated, and diluted 15-fold in buffer D [50 mM TRIS (pH 7.5), 20 mM NaCl, 2 mM DTT]. The diluted protein was then loaded onto a 5-mL Bioscale High Q column (Bio-Rad) that was pre-equilibrated with buffer D and eluted using buffer E [50 mM TRIS (pH 7.5), 1 M NaCl, 2 mM DTT] with a stepwise NaCl gradient of concentrations 40 mM, 100 mM, 500 mM, and 800 mM NaCl. Each step was set to 1.6 CV and 2-mL fractions were collected. PhdA eluted at a concentration of ~500 mM NaCl and fractions were yellow-brown. Purity of eluted fractions was confirmed by SDS-PAGE. Pooled fractions were concentrated and exchanged into assay buffer [50 mM TRIS (pH 7.5), 150 mM NaCl, 1 mM $MgCl_2$ (Sigma), 5 mM $(NH_4)_2SO_4$ (Sigma), 5 mM DTT] using a pre-equilibrated PD-10 column and stored at 4°C in a stoppered serum bottle. Protein concentration was determined using the Bradford assay. UV-visible spectra confirmed the presence of [4Fe-4S] clusters bound to the protein (Extended Data Figure 11~~8~~)[42].

For PhdB purification, strain AS019 (Extended Data Table 1) cell pellets were washed in buffer containing 50 mM TRIS (pH 7.5), 150 mM NaCl, and 0.5 mM dithionite. For purification, cell pellets were resuspended in buffer A [20 mM TRIS (pH 7.5), 200 mM NaCl, 1 mM EDTA (EMD Millipore), 1 mM DTT] and mixed with powdered protease inhibitors, chicken egg lysozyme (300 µg/mL) and DNaseI (10 µg/mL). This mixture was incubated for 20 minutes, followed by cell lysis with a French pressure cell under anaerobic conditions and clarification of the lysate as described for PhdA. The clarified lysate was filtered through a 0.45-µm filter (Millipore) and loaded on to a 5 mL-MBPTrap HP column (GE Healthcare) that was pre-equilibrated with buffer A. The column was then washed with 3 CV of buffer A to remove unbound proteins and eluted using a program consisting of a stepwise maltose gradient made by

mixing buffer A with buffer B [20 mM TRIS (pH 7.5), 200 mM NaCl, 1 mM EDTA, 10 mM maltose (Sigma), 1 mM DTT] using concentrations of 0.4 mM, 1 mM, 5 mM, and 8 mM maltose. Each step was set to 1.6 CV and 1-mL fractions were collected. PhdB eluted at a concentration of ~1 mM maltose and purity of fractions was confirmed by SDS-PAGE. Elution fractions were pooled and DTT was added to a final concentration of 2 mM and the protein was concentrated anaerobically as described for PhdA (except with a 50-kDa MWCO rather than 10-kDa MWCO). Concentrated protein was exchanged into assay buffer [50 mM TRIS (pH 7.5), 150 mM NaCl, 1 mM $MgCl_2$, 5 mM $(NH_4)_2SO_4$, 5 mM DTT)] using a pre-equilibrated PD-10 desalting column (GE Healthcare). Protein concentration was determined using the Bradford assay (Bio-Rad). During initial purifications, the identity of the protein was confirmed by Western blotting using HRP-conjugated anti-MBP antibody (New England Biolabs).

Anaerobic *in vitro* assays for PhdA activity with recombinant protein

In an anaerobic chamber at ambient temperature, 0.7 mM reconstituted PhdA was incubated in assay buffer [50 mM TRIS (pH 7.5), 150 mM NaCl, 1 mM $MgCl_2$, 5 mM $(NH_4)_2SO_4$, 5 mM DTT)] with 2 mM dithionite (Sigma) for 1 hour in 4-mL screw-capped glass vials (Supelco). This was followed by the addition of 2 mM SAM [*S*-(5'-adenosyl)-L-methionine chloride dihydrochloride; Sigma]. The reaction mixture (1.2 mL) was shaken at low speed on a tabletop orbital shaker. After initiation of the PhdA reaction by SAM addition, sampling was conducted from 0 to 180 min at 30-min intervals. Immediately upon sampling, 75 µL of reaction mixture was quenched by addition of 75 µL LC/MS grade methanol (Honeywell Research Chemicals, Muskegon, MI) and gentle bubbling of 0.5 mL of air (from a sealed serum bottle). Control reaction mixtures excluding PhdA were assayed in an identical manner. Post quenching, samples were centrifuged at 13,000 rpm for 15 min, then diluted in 50% (v/v) methanol in

LC/MS grade water (J.T. Baker, Phillipsburg, NJ) in preparation for LC/MS measurement. Replicates involved separate assays rather than multiple analyses of a given assay sample.

For analysis of methionine produced by PhdA activity with SAM, external standard quantification was performed with five-point calibration standards ranging from 0.25-10 μM methionine (Sigma) in 50/50 (v/v) methanol/water. Samples were run on an LC/MSD SL (Agilent, Santa Clara, CA) equipped with a model 1260 Infinity Binary Pump and operated in the electrospray ionization, positive-ion mode. The mobile phase initially flowed at 0.6 mL/min (0 - 13 min), and later at 1 mL/min (13-15 min), through a Kinetex HILIC column (2.6-μm particle size, 4.6-mm inner diameter x 50-mm length; Phenomenex, Torrance, CA). The initial mobile phase composition was 10 vol% A (20 mM ammonium acetate in water) and 90 vol% B (10 mM ammonium acetate in 90% acetonitrile, 10% water), which was decreased linearly to 70% B at 4 minutes, then decreased linearly to 40% B from 6 - 11.5 minutes, and then increased linearly to 90% B from 12 - 15 minutes to re-equilibrate the column to initial conditions. Sample injection volume was 2 μL. Source conditions included 3.5 kV capillary voltage, 250°C drying gas temperature, 12 L/min drying gas flow, and 25 psig nebulizer pressure. Data acquisition for methionine was in the selected ion monitoring (SIM) mode at *m/z* 150.2. Peak areas were integrated using Mass Hunter software (Agilent, version B.05.00).

Anaerobic *in vitro* assays for phenylacetate decarboxylase activity with recombinant PhdA and PhdB

Assays for phenylacetate decarboxylase activity were performed under strictly anaerobic conditions within a glove box. Assays, which were performed in 4-mL glass vials sealed with 13-mm diameter PTFE Mininert screw-cap valves (Sigma-Aldrich), contained 250 μM PhdA in assay buffer [50 mM TRIS (pH 7.5), 150 mM NaCl, 1 mM $MgCl_2$, 5 mM $(NH_4)_2SO_4$, 5 mM

DTT)], to which 2 mM dithionite was added and incubated for ~1 hour, followed by the addition of 2 mM SAM, 2.5 µM PhdB in assay buffer, and 2.5 mM phenylacetic acid-2-^{13}C in a final volume of 1 or 1.5 mL (depending on the specific experiment). Quantitative standards contained the same headspace/liquid ratios as assays and a dimensionless Henry's constant of 0.27[43] was used to calculate aqueous concentration. Negative controls were run concurrently and were identical except for the absence of SAM (Figure 3b) or other conditions specified in Extended Figure 4. The vials were shaken on a tabletop orbital shaker at low speed. Gaseous headspace samples (100 µL) were taken within the glove box using a 500-µL gastight syringe (Sample-Lok series A-2; Sigma-Aldrich) and analyzed immediately by GC/MS, as described previously[8]. Briefly, toluene was analyzed by static headspace, electron ionization (EI) GC/MS using a model 7890A GC (Agilent, Santa Clara, CA) with a DB-5 fused silica capillary column (30-m length, 0.25-mm inner diameter, 0.25-µm film thickness; Agilent) coupled to an HP 5975C series quadrupole mass spectrometer. As described elsewhere[8], the identity of [*methyl*-^{13}C]toluene was confirmed with the expected *m/z* 93/92 ratio of 0.6. Replicates involved separate assays rather than multiple analyses of a given assay sample. In assays testing whether PhdB could decarboxylate *p*-hydroxyphenylacetate to *p*-cresol, conditions were as described above except that equimolar amounts (2.5 mM) of *p*-hydroxyphenylacetic acid (Sigma) and phenylacetic acid-2-^{13}C were added, and GC/MS analysis of *p*-cresol in 1-µL liquid injections of concentrated hexane extracts were conducted as described previously[8]. The identity of *p*-cresol was assessed using retention time and the expected *m/z* 108/107 ratio of 0.83 based on authentic standards.

PCR amplification of *phd* gene cluster from genomic DNA from lake sediment culture

phdA, *phdB*, and an adjacent putative transcription factor were PCR-amplified from genomic DNA extracted from the lake sediment community using primers shown in Extended

Data Table 2. Primer design was guided in part by partial gene sequences available from metagenomes (IMG Taxon ID 2100351000 and 3300001865). Amplified and gel-purified DNA was sequenced by Genewiz.

Construction of maximum likelihood tree of glycyl radical enzymes in sewage-derived culture

The maximum-likelihood tree in Fig. 1 encompasses protein sequences of putative glycyl radical enzymes (GREs) detected in the sewage culture metagenome (IMG Taxon ID 3300001865) based on BLASTP[31] searches against known GREs (> 30% sequence identity), searches for the glycyl radical motif (FIMO[44]), and a minimum length of 171 amino acids (not all were full length). The following model sequences were also included in the tree to provide context (accession numbers in parenthesis): PflB (GenBank: NP_415423), HpdB (GenBank: AJ543425.1), CsdB (GenBank: ABB05046.1), CutC (PDB: 5A0Z), NrdD (GenBank: NP_418659), and Gdh (PDB: 1R8W). The collected set of model and putative GRE sequences (*n*=81, mean = 675±194 aa) were aligned using MUSCLE v. 3.8.31[45]. The resulting MSA was screened for ambiguous C and N termini as well as columns with >97% gaps. The final alignment spanned 1138 columns. A maximum likelihood phylogenetic tree was inferred with RAxML v. 7.6.3[46], under the LG plus Gamma model of evolution as follows:

raxmlHPC-PTHREADS-SSE3 -# 50 -m PROTGAMMAGTR -p 777 -x 2000 -f a

The tree was constructed with iTOL[47].

Binning of sewage culture metagenomes and recovery of *Acidobacteria* strain Tolsyn genome

For binning, two groups of sewage metagenomes (Group 1 from SRA accession numbers SRP077640, SRP072654, and SRP099295 and Group 2 from SRA accession numbers

576SRP105442 and SRP105443) were separately co-assembled using metaSPAdes v3.6[48] with the 577“--careful" option. The two co-assemblies were separately binned using MaxBin 2.0[49] with 578default parameters (-min_contig_len 1000). The *Acidobacteria* strain Tolsyn bins were separately 579identified within the two co-assemblies, and scaffolds that were shared (with >98% identity) 580were selected to constitute the draft *Acidobacteria* genome. The scaffolds were further refined by 581mapping against the hybrid assemblies of the sewage sludge samples (IMG Taxon ID 5823300017643, 3300017642, and 3300017814) and extracting scaffolds that unambiguously 583connected two or more sequences in the draft *Acidobacteria* genome. Genes were predicted from 584the genome using Prodigal (parameter: -p meta)[50]. Amino acid sequence identity between the 585draft Tolsyn genome and the *Ca.* Koribacter versatilis genome was carried out by comparing 586predicted proteins from the two genomes using BLASTP[31] with an e-value cutoff of 1e-10 and 587coverage cutoff 0.4. Annotation was performed by matching identical genes identified by the 588IMG pipeline (IMG Taxon ID 3300001865) using BLASTP with minimum amino acid identity 589set to 95% and minimum coverage set to 40%; the best matching IMG annotations were then 590assigned for those genes. CheckM software[51] reported that the genome was 96.35% complete 591with a contamination ratio of 1.69%. The circular genome plot (Fig. 6a) was made using 592Circos[52]. The 16S rRNA gene was identified as follows. A partial 16S rRNA gene (756 bp) was 593identified in a 1.7-kb scaffold and was 100% identical to a 16S rRNA gene identified from 16S 594rRNA iTag analysis: *Acidobacteria* OTU (Operational Taxonomic Unit) #9 (Supplementary Data 595File 3). When OTU9 was used as query sequence for BLASTN searches of the sewage culture 596metagenome (IMG Taxon ID 3300001865), it had a 100% match with scaffold 597JGI2065J20421_1000212, which contained a 1382-bp 16S rRNA gene

(JGI2065J20421_10002126). As a result, the partial 16S rRNA gene in the *Acidobacteria* strain Tolsyn genome was replaced by the 1382-bp 16S rRNA gene.

Construction of phylogenetic trees for *Acidobacteria* strain Tolsyn

The 16S rRNA tree (Extended Data Fig. 96) was constructed by aligning selected 16S rRNA gene sequences using MUSCLE[45] and then applying FastTree[53] to the alignment file. The concatenated protein tree (Fig. 6b) was constructed with ezTree (https://github.com/yuwwu/ezTree; manuscript under review), a pipeline for identifying single-copy marker genes from a collection of complete or draft genomes and using the marker genes to generate a concatenated protein tree.

Molecular modeling of PhdB in complex with its phenylacetate substrate

A molecular model of PhdB (Extended Figure 8) was created based on homology modeling of three-dimensional protein structures implemented in the program SWISS-MODEL[54]. The GRE 1,2-propanediol dehydratase from *Roseburia inulinivorans* (PDB ID: 5I2A), which shares 32% sequence identity with PhdB, was used as a template to generate the molecular model of PhdB. Superposition of the CsdB in complex with *p*-hydroxyphenylacetate (PDB ID: 2YAJ)[28] against the molecular model of PhdB with the program COOT[55] was used to extract the binding position of phenylacetate. A structure idealization of PhdB-phenylacetate using REFMAC[56] enabled the final molecular model of the complex. The overall stereochemical quality of the final models was assessed using the program MolProbity[57].

Data Availability

Data that support the findings of this study are available within the paper, its supplementary information files, and data repositories cited therein [including JGI's IMG-M site (https://img.jgi.doe.gov/cgi-bin/mer/main.cgi), NCBI's Sequence Read Archive

621(https://trace.ncbi.nlm.nih.gov/Traces/sra/sra.cgi), and the public version of the JBEI Registry 622(https://public-registry.jbei.org), which contains strains, plasmids, and their associated 623information].

References

Galperin, M. Y. & Koonin, E. V. From complete genome sequence to 'complete' understanding? *Trends Biotechnol.* **28**, 398-406, doi:10.1016/j.tibtech.2010.05.006 (2010).

Gerlt, J. A. *et al.* The Enzyme Function Initiative. *Biochemistry* **50**, 9950-9962, doi:10.1021/bi201312u (2011).

Anton, B. P. *et al.* The COMBREX project: design, methodology, and initial results. *PLoS Biol.* **11**, e1001638, doi:10.1371/journal.pbio.1001638 (2013).

Lespinet, O. & Labedan, B. Orphan enzymes? *Science* **307**, 42, doi:10.1126/science.307.5706.42a (2005).

Sorokina, M., Stam, M., Medigue, C., Lespinet, O. & Vallenet, D. Profiling the orphan enzymes. *Biol. Direct* **9**, 10, doi:10.1186/1745-6150-9-10 (2014).

McKenna, R. & Nielsen, D. R. Styrene biosynthesis from glucose by engineered *E. coli*. *Metab. Eng.* **13**, 544-554, doi:10.1016/j.ymben.2011.06.005 (2011).

Jüttner, F. & Henatsch, J. J. Anoxic hypolimnion is a significant source of biogenic toluene. *Nature* **323**, 797-798 (1986).

Zargar, K. *et al. In vitro* characterization of phenylacetate decarboxylase, a novel enzyme catalyzing toluene biosynthesis in an anaerobic microbial community. *Scientific Reports* **6**, 31362, doi:10.1038/srep31362 (2016).

Fischer-Romero, C., Tindall, B. J. & Juttner, F. *Tolumonas auensis* gen. nov., sp. nov., a toluene-producing bacterium from anoxic sediments of a freshwater lake. *Int. J. Syst. Bacteriol.* **46**, 183-188, doi:10.1099/00207713-46-1-183 (1996).

Pons, J. L., Rimbault, A., Darbord, J. C. & Leluan, G. [Biosynthesis of toluene in *Clostridium aerofoetidum* strain WS]. *Ann. Microbiol. (Paris)* **135B**, 219-222 (1984).

Akhtar, M. K., Turner, N. J. & Jones, P. R. Carboxylic acid reductase is a versatile enzyme for the conversion of fatty acids into fuels and chemical commodities. *Proc. Natl. Acad. Sci. U S A* **110**, 87-92, doi:10.1073/pnas.1216516110 (2013).

Schirmer, A., Rude, M. A., Li, X., Popova, E. & del Cardayre, S. B. Microbial biosynthesis of alkanes. *Science* **329**, 559-562, doi:10.1126/science.1187936 (2010).

Selmer, T. & Andrei, P. I. *p*-Hydroxyphenylacetate decarboxylase from *Clostridium difficile*. A novel glycyl radical enzyme catalysing the formation of *p*-cresol. *Eur. J. Biochem.* **268**, 1363-1372 (2001).

Yu, L., Blaser, M., Andrei, P. I., Pierik, A. J. & Selmer, T. 4-Hydroxyphenylacetate decarboxylases: properties of a novel subclass of glycyl radical enzyme systems. *Biochemistry* **45**, 9584-9592, doi:10.1021/bi060840b (2006).

Selmer, T., Pierik, A. J. & Heider, J. New glycyl radical enzymes catalysing key metabolic steps in anaerobic bacteria. *Biol. Chem.* **386**, 981-988, doi:10.1515/BC.2005.114 (2005).

Shisler, K. A. & Broderick, J. B. Glycyl radical activating enzymes: structure, mechanism, and substrate interactions. *Arch. Biochem. Biophys.* **546**, 64-71, doi:10.1016/j.abb.2014.01.020 (2014).

Leuthner, B. *et al.* Biochemical and genetic characterization of benzylsuccinate synthase from *Thauera aromatica*: a new glycyl radical enzyme catalysing the first step in anaerobic toluene metabolism. *Mol. Microbiol.* **28**, 615-628 (1998).

66918 O'Brien, J. R. *et al.* Insight into the mechanism of the B12-independent glycerol
670 dehydratase from *Clostridium butyricum*: preliminary biochemical and structural
671 characterization. *Biochemistry* **43**, 4635-4645, doi:10.1021/bi035930k (2004).
67219 Beller, H. R. & Spormann, A. M. Substrate range of benzylsuccinate synthase from
673 *Azoarcus* sp. strain T. *FEMS Microbiol. Lett.* **178**, 147-153 (1999).
67420 Becker, A. *et al.* Structure and mechanism of the glycyl radical enzyme pyruvate formate-
675 lyase. *Nat. Struct. Biol.* **6**, 969-975, doi:10.1038/13341 (1999).
67621 Larsson, K. M., Andersson, J., Sjoberg, B. M., Nordlund, P. & Logan, D. T. Structural
677 basis for allosteric substrate specificity regulation in anaerobic ribonucleotide reductases.
678 *Structure* **9**, 739-750 (2001).
67922 Heider, J., Spormann, A. M., Beller, H. R. & Widdel, F. Anaerobic bacterial metabolism
680 of hydrocarbons. *FEMS Microbiology Reviews* **22**, 459-473 (1998).
68123 Feliks, M., Martins, B. M. & Ullmann, G. M. Catalytic mechanism of the glycyl radical
682 enzyme 4-hydroxyphenylacetate decarboxylase from continuum electrostatic and
683 QC/MM calculations. *J. Am. Chem. Soc.* **135**, 14574-14585, doi:10.1021/ja402379q
684 (2013).
68524 Kalnins, G. *et al.* Structure and function of CutC choline lyase from human microbiota
686 bacterium *Klebsiella pneumoniae*. *J Biol Chem* **290**, 21732-21740,
687 doi:10.1074/jbc.M115.670471 (2015).
68825 Craciun, S. & Balskus, E. P. Microbial conversion of choline to trimethylamine requires a
689 glycyl radical enzyme. *Proc. Natl. Acad. Sci. U S A* **109**, 21307-21312,
690 doi:10.1073/pnas.1215689109 (2012).

69126 Levin, B. J. *et al.* A prominent glycyl radical enzyme in human gut microbiomes
692 metabolizes *trans*-4-hydroxy-l-proline. *Science* **355**, doi:10.1126/science.aai8386 (2017).
69327 Funk, M. A., Marsh, E. N. & Drennan, C. L. Substrate-bound structures of
694 benzylsuccinate synthase reveal how toluene is activated in anaerobic hydrocarbon
695 degradation. *J. Biol. Chem.* **290**, 22398-22408, doi:10.1074/jbc.M115.670737 (2015).
69628 Martins, B. M. *et al.* Structural basis for a Kolbe-type decarboxylation catalyzed by a
697 glycyl radical enzyme. *J. Am. Chem. Soc.* **133**, 14666-14674, doi:10.1021/ja203344x
698 (2011).
69929 Kielak, A. M., Barreto, C. C., Kowalchuk, G. A., van Veen, J. A. & Kuramae, E. E. The
700 Ecology of *Acidobacteria*: Moving beyond Genes and Genomes. *Front. Microbiol.* **7**,
701 744, doi:10.3389/fmicb.2016.00744 (2016).
70230 Ward, N. L. *et al.* Three genomes from the phylum *Acidobacteria* provide insight into the
703 lifestyles of these microorganisms in soils. *Appl. Environ. Microbiol.* **75**, 2046-2056,
704 doi:10.1128/AEM.02294-08 (2009).
70531 Altschul, S. F., Gish, W., Miller, W., Myers, E. W. & Lipman, D. J. Basic local alignment
706 search tool. *J. Mol. Biol.* **215**, 403-410, doi:10.1016/S0022-2836(05)80360-2 (1990).
70732 Dawson, L. F., Stabler, R. A. & Wren, B. W. Assessing the role of *p*-cresol tolerance in
708 *Clostridium difficile*. *J. Med. Microbiol.* **57**, 745-749, doi:10.1099/jmm.0.47744-0
709 (2008).
71033 Schneider, S., Mohamed, M. E. S. & Fuchs, G. Anaerobic metabolism of L-phenylalanine
711 via benzoyl-CoA in the denitrifying bacterium *Thauera aromatica*. . *Arch. Microbiol.*
712 **168**, 310-320 (1997).

71334 Carmona, M. *et al.* Anaerobic catabolism of aromatic compounds: a genetic and genomic
714 view. *Microbiol. Mol. Biol. Rev.* **73**, 71-133, doi:10.1128/MMBR.00021-08 (2009).
71535 Molenaar, D., Bosscher, J. S., ten Brink, B., Driessen, A. J. & Konings, W. N. Generation
716 of a proton motive force by histidine decarboxylation and electrogenic
717 histidine/histamine antiport in *Lactobacillus buchneri*. *J Bacteriol* **175**, 2864-2870
718 (1993).
71936 Pereira, C. I., Matos, D., San Romao, M. V. & Crespo, M. T. Dual role for the tyrosine
720 decarboxylation pathway in *Enterococcus faecium* E17: response to an acid challenge and
721 generation of a proton motive force. *Appl Environ Microbiol* **75**, 345-352,
722 doi:10.1128/AEM.01958-08 (2009).
72337 Beller, H. R., Legler, T. C. & Kane, S. R. Genetic manipulation of the obligate
724 chemolithoautotrophic bacterium *Thiobacillus denitrificans*. *Methods Mol. Biol.* **881**, 99-
725 136, doi:10.1007/978-1-61779-827-6_5 (2012).
72638 Huntemann, M. *et al.* The standard operating procedure of the DOE-JGI Microbial
727 Genome Annotation Pipeline (MGAP v.4). *Stand. Genomic Sci.* **10**, 86,
728 doi:10.1186/s40793-015-0077-y (2015).
72939 Edgar, R. C. UPARSE: highly accurate OTU sequences from microbial amplicon reads.
730 *Nat. Methods* **10**, 996-998, doi:10.1038/nmeth.2604 (2013).
73140 Quast, C. *et al.* The SILVA ribosomal RNA gene database project: improved data
732 processing and web-based tools. *Nucleic Acids Res.* **41**, D590-596,
733 doi:10.1093/nar/gks1219 (2013).
73441 Studier, F. W. Protein production by auto-induction in high density shaking cultures.
735 *Protein Expr. Purif.* **41**, 207-234 (2005).

Gao, H. *et al. Arabidopsis thaliana* Nfu2 accommodates [2Fe-2S] or [4Fe-4S] clusters and is competent for *in vitro* maturation of chloroplast [2Fe-2S] and [4Fe-4S] cluster-containing proteins. *Biochemistry* **52**, 6633-6645, doi:10.1021/bi4007622 (2013).

Mackay, D. & Shiu, W. Y. A critical review of Henry's Law constants for chemicals of environmental interest. *Journal of Physical and Chemical Reference Data* **10**, 1175-1199 (1981).

Grant, C. E., Bailey, T. L. & Noble, W. S. FIMO: scanning for occurrences of a given motif. *Bioinformatics* **27**, 1017-1018, doi:10.1093/bioinformatics/btr064 (2011).

Edgar, R. C. MUSCLE: multiple sequence alignment with high accuracy and high throughput. *Nucleic Acids Res.* **32**, 1792-1797, doi:10.1093/nar/gkh340 (2004).

Stamatakis, A. RAxML version 8: a tool for phylogenetic analysis and post-analysis of large phylogenies. *Bioinformatics* **30**, 1312-1313, doi:10.1093/bioinformatics/btu033 (2014).

Letunic, I. & Bork, P. Interactive tree of life (iTOL) v3: an online tool for the display and annotation of phylogenetic and other trees. *Nucleic Acids Res.* **44**, W242-245, doi:10.1093/nar/gkw290 (2016).

Bankevich, A. *et al.* SPAdes: a new genome assembly algorithm and its applications to single-cell sequencing. *J. Comput. Biol.* **19**, 455-477, doi:10.1089/cmb.2012.0021 (2012).

Wu, Y. W., Simmons, B. A. & Singer, S. W. MaxBin 2.0: an automated binning algorithm to recover genomes from multiple metagenomic datasets. *Bioinformatics* **32**, 605-607, doi:10.1093/bioinformatics/btv638 (2016).

Hyatt, D. *et al.* Prodigal: prokaryotic gene recognition and translation initiation site identification. *BMC bioinformatics* **11**, 119, doi:10.1186/1471-2105-11-119 (2010).

Parks, D. H., Imelfort, M., Skennerton, C. T., Hugenholtz, P. & Tyson, G. W. CheckM: assessing the quality of microbial genomes recovered from isolates, single cells, and metagenomes. *Genome Res.* **25**, 1043-1055, doi:10.1101/gr.186072.114 (2015).

Krzywinski, M. *et al.* Circos: an information aesthetic for comparative genomics. *Genome Res.* **19**, 1639-1645, doi:10.1101/gr.092759.109 (2009).

Price, M. N., Dehal, P. S. & Arkin, A. P. FastTree: computing large minimum evolution trees with profiles instead of a distance matrix. *Mol. Biol. Evol.* **26**, 1641-1650, doi:10.1093/molbev/msp077 (2009).

Biasini, M. *et al.* SWISS-MODEL: modelling protein tertiary and quaternary structure using evolutionary information. *Nucleic acids research* **42**, W252-258, doi:10.1093/nar/gku340 (2014).

Emsley, P. & Cowtan, K. Coot: model-building tools for molecular graphics. *Acta Crystallogr D Biol Crystallogr* **60**, 2126-2132, doi:10.1107/S0907444904019158 (2004).

Vagin, A. A. *et al.* REFMAC5 dictionary: organization of prior chemical knowledge and guidelines for its use. *Acta Crystallogr D Biol Crystallogr* **60**, 2184-2195, doi:10.1107/S0907444904023510 (2004).

Davis, I. W. *et al.* MolProbity: all-atom contacts and structure validation for proteins and nucleic acids. *Nucleic acids research* **35**, W375-383, doi:10.1093/nar/gkm216 (2007).

Sievers, F. *et al.* Fast, scalable generation of high-quality protein multiple sequence alignments using Clustal Omega. *Mol. Syst. Biol.* **7**, 539, doi:10.1038/msb.2011.75 (2011).

Supplementary Information is linked to the online version of the paper at www.nature.com/nature.

Acknowledgments

We thank the following people from JBEI, LBNL, and JGI for their valuable contributions to this work: Ulas Karaoz, Nathan Hillson, Andy DeGiovanni, ~~Paul Adams, Jose Henrique Pereira,~~ Ee-Been Goh, Edward Baidoo, Xi Wang, Shi Wang, Patrick Sorensen, Suzan Yilmaz, Garima Goyal, Joshua Heazlewood, Tijana Glavina del Rio, Stephanie Malfatti, Emiley Eloe-Fadrosh, and Adam Rivers; we also thank Michelle Salemi (UC Davis Genome Center, Proteomics Core Facility).

This work was part of the DOE Joint BioEnergy Institute (http://www.jbei.org) supported by the U. S. Department of Energy, Office of Science, Office of Biological and Environmental Research, through contract DE-AC02-05CH11231 between Lawrence Berkeley National Laboratory and the U. S. Department of Energy. Work conducted by the Department of Energy Joint Genome Institsute, a DOE Office of Science User Facility, is supported by the Office of Science of the U.S. Department of Energy under Contract No. DE-AC02-05CH11231

Author Contributions

H.R.B., A.V.R., K.Z. and R.M.S. conceived of and designed the experiments. A.V.R., K.Z., H.R.B., A.K.S., and R.S. performed the experiments. H.R.B., Y.W.W., and A.V.R. analyzed the data. S.G.T. oversaw metagenomic data production and C.J.P. oversaw metaproteomic data production. The manuscript was written by H.R.B. (primarily) and all authors, including J.D.K., contributed to refining the text.

804

805**Author Information**

806Reprints and permissions information is available at www.nature.com/reprints. J.D.K. has a

807financial interest in Amyris and Lygos. Correspondence and requests for materials should be

808addressed to H.R.B (HRBeller@lbl.gov).

809

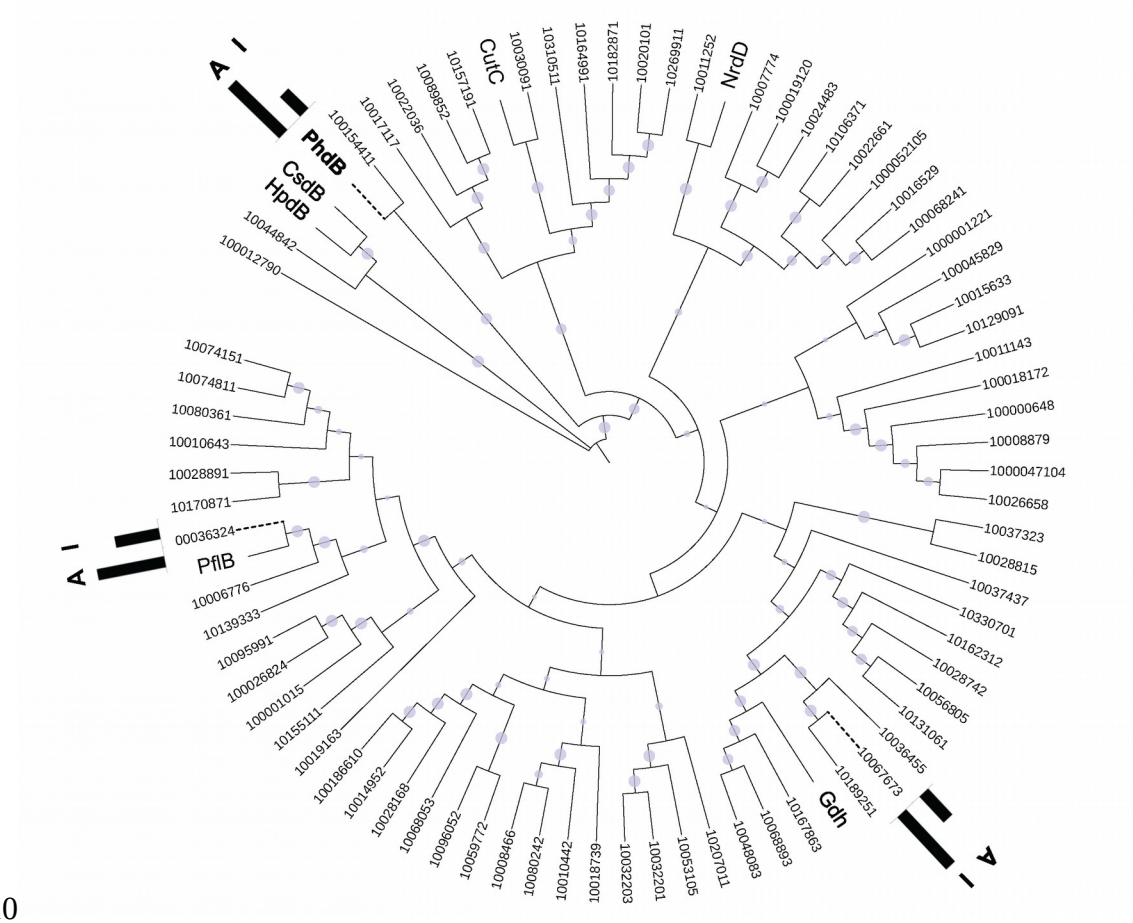

Figure 1 | Glycyl radical enzymes encoded in the toluene-producing sewage culture metagenome and their association with *in vitro* toluene synthase activity. This maximum-likelihood tree is based on protein sequences of putative glycyl radical enzymes (GREs) detected in the sewage-derived metagenome [IMG Taxon ID 3300001865 on JGI's IMG-M site (https://img.jgi.doe.gov/cgi-bin/mer/main.cgi)]. Numerical values on the leaves represent locus tags in the metagenome from which the prefix "JGI2065J20421_" has been truncated for brevity. Leaves with protein names rather than locus tags are known GREs provided for context (see Methods for details). The leaf marked PhdB represents the GRE characterized in this study. Leaves with dashed lines represent proteins detected by LC/MS/MS in active FPLC fractions, and the histograms on these leaves represent the maximum abundance of this protein in (A) the two most active fractions and (I) the two flanking inactive or less active fractions (Supplementary Data File 1); histograms are normalized to the greatest of the A and I values. Purple circles on leaves represent bootstrap support values for each node (largest symbols are 100).

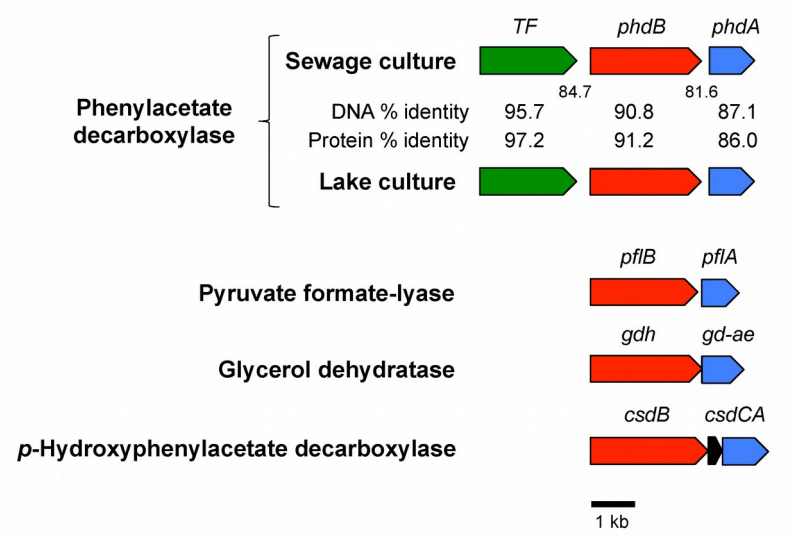

Figure 2 | Homologous ~~toluene synthas~~phenylacetate decarboxylase~~e~~ gene clusters from sewage and lake sediment cultures. *phdB*, phenylacetate decarboxylase (a glycyl radical enzyme); *phdA*, a cognate activating enzyme for *phdB*; *TF*, putative transcription factor. Sequence identity is shown for the coding sequences as well as the two intergenic regions. Gene clusters for selected GREs (in red) and their cognate activating enzymes (in blue) are shown for comparison, including pyruvate formate-lyase (*pflB*, *pflA*), glycerol dehydratase (*gdh*, *gd-ae*), and *p*-hydroxyphenylacetate decarboxylase (*csdB*, *csdC*, *csdA*). A 1-kb scale bar is included.

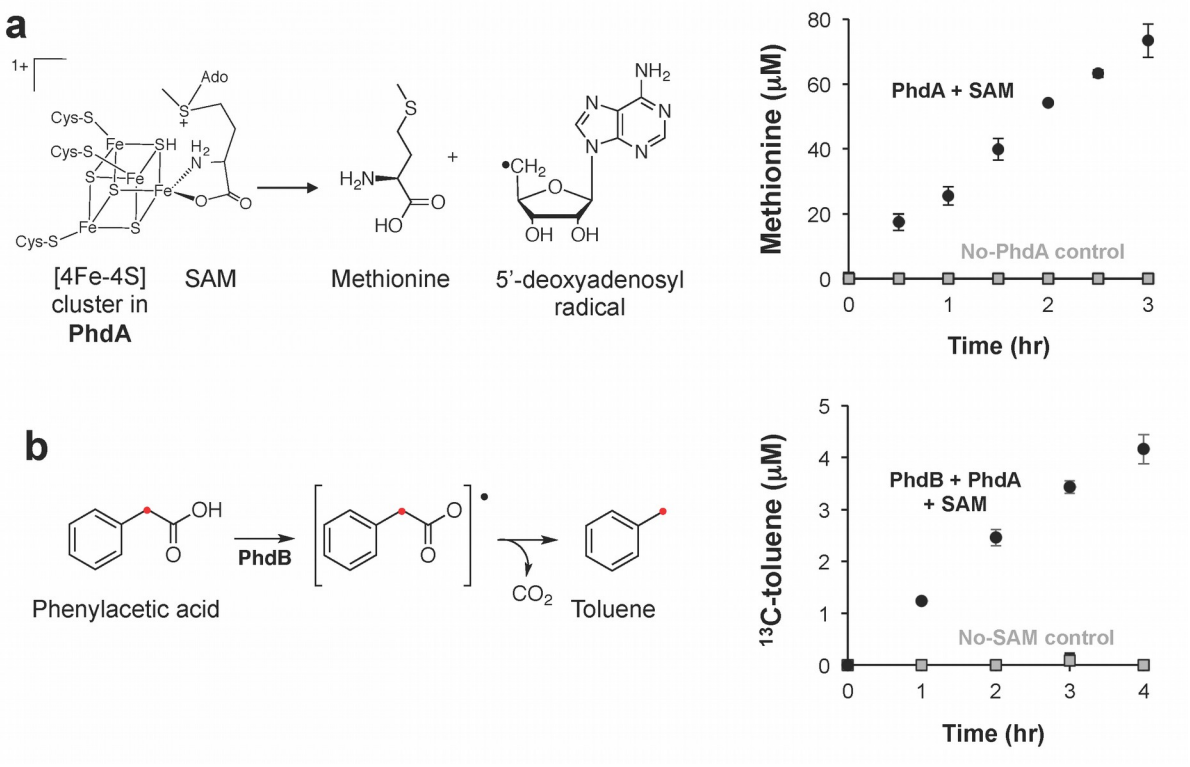

Figure 3 | Reactions catalyzed by PhdA and PhdB. a, proposed reaction of PhdA with SAM, as supported *in vitro* by methionine production by re-constituted and purified recombinant PhdA (black circles). Controls without PhdA are also shown (gray squares). **b**, proposed reaction of PhdB with phenylacetic acid-2-^{13}C, as supported *in vitro* by [*methyl*-^{13}C]toluene production by partially purified PhdB in combination with PhdA and SAM (black circles). Controls without SAM are also shown (gray squares). ^{13}C-labeled C atoms in the proposed reaction are highlighted with a red circle. Data points represent means and error bars represent one standard deviation (n=3). Experiments demonstrating PhdA-catalyzed production of methionine from SAM were replicated ~~twice~~ three times and experiments demonstrating labeled toluene production from labeled phenylacetate in the presence of PhdB and PhdA were performed 6 times (four times with no-SAM negative controls).

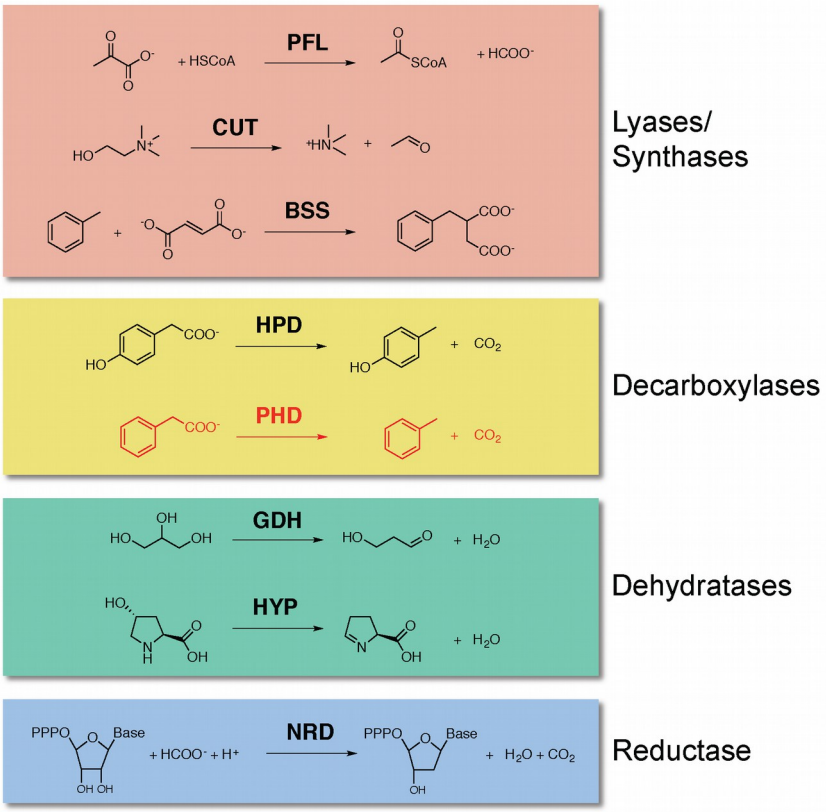

Figure 4 | **Reactions catalyzed by characterized GREs.** PFL, pyruvate formate-lyase; CUT, choline trimethylamine-lyase; BSS, benzylsuccinate synthase; HPD, *p*-hydroxyphenylacetate decarboxylase; PHD, phenylacetate decarboxylase (this study); GDH, glycerol dehydratase; HYP, *trans*-4-hydroxy-L-proline dehydratase; and NRD, anaerobic ribonucleotide reductase.

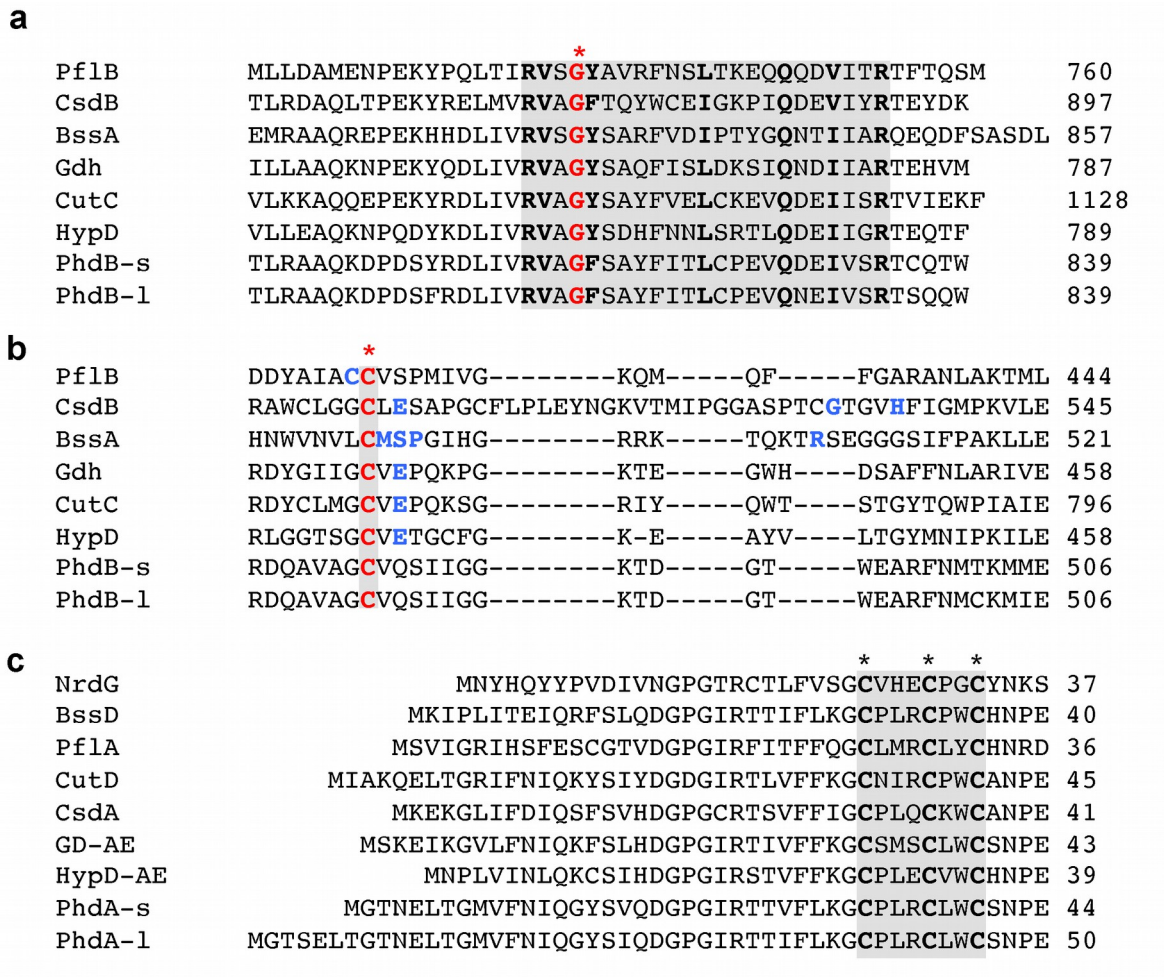

Figure 5 | **Multiple sequence alignments comparing PhdB and PhdA with other glycyl radical enzymes and glycyl radical activating enzymes, respectively. a,** C-terminal region of GREs containing the conserved glycyl radical motif, with the glycyl radical site highlighted in red with an asterisk and other conserved residues in bold. **b**, mid-sequence region of GREs containing conserved, active-site cysteine residue (which bears the thiyl radical that interacts with the substrate), highlighted in red with an asterisk, along with other conserved residues shown in blue. **c**, N-Terminal region of activating enzymes highlighting the CxxxCxxC motif (highlighted with asterisks) coordinating with the [4Fe-4S] cluster. Sequences used in these alignment comparisons include the following GREs and AEs [PDB (Protein Data Bank) or GenBank accession number]: PflB (GenBank: NP_415423), PflA (GenBank: NP_415422), CsdB (GenBank: ABB05046.1), CsdA (GanBank: 2580384209), BssA (PDB: 4PKC:A), BssD (GenBank: CAA05050.2), Gdh (PDB: 1R8W), GD-AE (GenBank: AAM54729), CutC (PDB: 5A0Z), CutD (GenBank: EPO20361.1), HypD (UniProt: A0A031WDE4), HypD-AE (UniProt: A0A069AMK2), NrdG (GenBank: NP_418658). The “s” and “l” suffixes for PhdB and PhdA stand for sewage and lake, respectively. Alignment was performed with Clustal Omega[58].

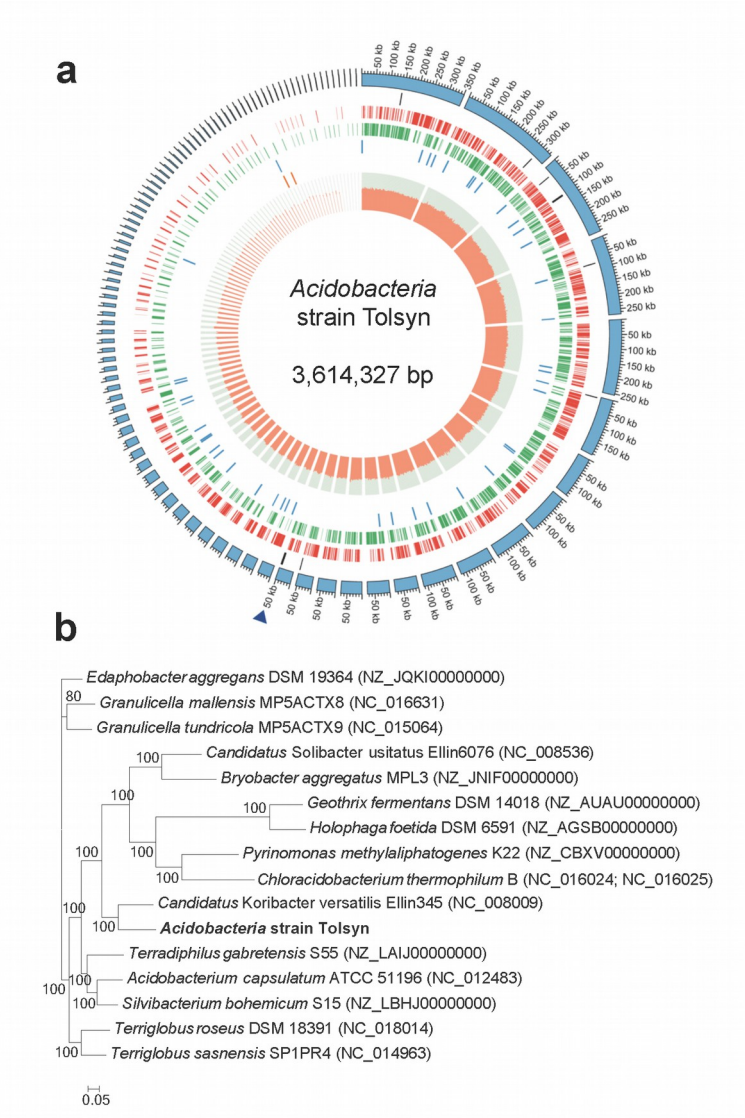

Figure 6 | Characterization of the putatively toluene-producing *Acidobacterium* strain Tolsyn based on its recovered genome. **a**, schematic circular diagram of the genome, with contigs in size order, displaying contigs and their corresponding lengths (outer ring), genes encoding radical-related enzymes (second ring; the contig containing *phdA* and *phdB* is indicated with a filled triangle), genes on the forward strand (third ring), genes on the reverse strand (fourth ring), tRNA genes (fifth ring), rRNA genes (sixth ring), and GC content (seventh ring; GC is averaged every 1000 bp and is represented as orange, whereas AT is light green). **b**, Phylogenetic relationships among *Acidobacterium* strain Tolsyn and the most closely related *Acidobacteria* sequenced isolates based upon 129 concatenated marker proteins (GenBank accession numbers for species are shown in the tree). Numbers at nodes represent bootstrap support values. The scale bar represents substitution rate per site.